Kinetic and potential mechanisms for deuteron production in heavy-ion collisions within the PHQMD transport approach

G. Coci[1][2][*], S. Glaessel[3], V. Kireyeu[2][8], J. Aichelin[4][5],
E. Bratkovskaya[2][6][7], C. Blume[3] and V. Voronyuk[2][8]

[1] *Department of Physics and Astronomy "E. Majorana", University of Catania*
   Via S. Sofia 64, 1-95123 Catania, Italy
[2] *Helmholtz Research Academy Hessen for FAIR (HFHF),GSI Helmholtz Center for Heavy*
   Ion Physics, Campus Frankfurt - 60438 Frankfurt, Germany
[3] *Institute für Kernphysik - Max-von-Laue-Str. 1, 60438 Frankfurt, Germany*
[4] *SUBATECH, Université de Nantes, IMT Atlantique, IN2P3/CNRS - 4 rue Alfred Kastler,*
   44307 Nantes cedex 3, France
[5] *Frankfurt Institute for Advanced Studies - Ruth Moufang Str. 1, 60438 Frankfurt, Germany*
[6] *GSI Helmholtzzentrum für Schwerionenforschung GmbH - Planckstr. 1, 64291 Darmstadt,*
   Germany
[7] *Institut für Theoretische Physik, Johann Wolfgang Goethe University - Max-von-Laue-Str. 1,*
   60438 Frankfurt, Germany
[8] *Joint Institute for Nuclear Research - Joliot-Curie 6, 141980 Dubna, Moscow Region, Russia*

Summary. — This study explores the dynamical formation of deuterons in heavy-ion collisions using the Parton-Hadron-Quantum-Molecular Dynamics (PHQMD) approach. Two production mechanisms are investigated: "kinetic" production via "catalytic" reactions and "potential" interactions from nucleon attractive forces. Our analysis thoroughly examines all isospin channels for various reactions and considers deuteron finite-size properties. Results show that accounting for deuteron quantum properties significantly reduces the kinetic contribution in dense medium typical of heavy-ion collisions. Furthermore, by identifying potential deuterons with an advanced Minimum Spanning Tree (aMST) method, we obtain a satisfactory agreement with available experimental data.

1. – Introduction

Understanding the mechanisms behind the formation of weakly bound clusters, like the deuteron (d), in heavy-ion collisions (HICs) remains a significant enigma in the field both experimentally and theoretically, that has been named as "ice in the fire" puzzle. The formation of deuterons and other cluster species at bombarding energies above 1

(*) E-mail: gabriele.coci@dfa.unict.it.

AGeV up to the highest energies reached at Relativistic Heavy-Ion Collider (RHIC) and Large Hadron Collider (LHC) facilities has been modeled by two well-known approaches:

- The statistical model posits that hadrons originate from a globally equilibrated thermal source, defined by temperature T, baryon chemical potential μ_B, and fixed volume V. These parameters are determined by fitting the multiplicity of various hadrons at the chemical freeze-out. Remarkably, the observed cluster multiplicities are also captured by the same (T, μ_B, V) values. This model assumes that the expansion of the system does not alter the number of clusters, providing a framework for understanding particle emission at the chemical freeze-out.

- The coalescence approach assumes that a proton and a neutron form a deuteron if their distance in coordinate and momentum space is smaller than some parameters (r_{coal}, p_{coal}). Such distance is evaluated at kinetic freeze-out, textiti.e. when the last nucleon of the pair undergoes its final elastic collision. Various adaptations of the coalescence model exist, with some of them involving the projection of nucleon phase-space distribution functions onto the Wigner density of the deuteron, typically represented by a Gaussian distribution.

Both models provide good description of mid-rapidity measurements at various energies. However, they suffer from limiting the production of clusters to some fixed time of HICs evolution, thus preventing the possibility of investigating *when and where* the observed clusters are actually formed. In order to understand the microscopic origin of cluster formation, two dynamical mechanisms have been proposed:

i) The Minimum Spanning Tree (MST) method was initially developed to analyze fragments originating from both the projectile and target regions. Subsequently, it has been adapted for the study of mid-rapidity clusters [2]. This method operates under the assumption that, at the end of the heavy-ion reaction, two nucleons are considered part of a cluster if their distance falls within a radius $r_{clus} \leq 4$ fm, which is comparable to the range of the nucleon-nucleon interaction.

ii) The production (and disintegration) of deuteron by the "elementary" reaction $pnN \leftrightarrow dN$ (*nucleon catalysis*) was studied for the first time by Kapusta and collaborators at low energy HICs. More recently, it has been proposed in ref. [7] that at relativistic HICs the *pion catalyis*, textiti.e. $pn\pi \leftrightarrow d\pi$, becomes more dominant at mid-rapidity due to the large abundance of pions. In ref. [7] the $3 \to 2$ inelastic reaction has been approximated as a sequence of more simple $2 \to 2$ processes by employing a fictitious dibaryon resonance, whose mass and width parameters were tuned to reproduce the total inclusive cross section for πd inelastic scattering. Later in ref. [8], this numerical artifact has been replaced by multi-particle reactions implemented within the covariant rate formalism, which has been firstly developed in ref. [9] for studying baryon-antibaryon production. However, in these studies only reactions of the type $pn\pi^+ \leftrightarrow d\pi^+$, without inclusion of isospin degrees of freedom through charge exchange, have been considered and, above all, the deuteron, which has a radius of about 2 fm, has always been treated as a point-like particle.

2. – Model

In this study we make use of the Parton-Hadron-Quantum-Molecular-Dynamics (PHQMD), a robust many-body transport framework for studying hadrons and cluster production in HICs [2,3], which unifies two well-established kinetic approaches:

  i) In the Quantum Molecular Dynamics (QMD) approach [4] the baryons are represented by single-particle wave functions characterized by Gaussian distributions in coordinate and momentum space with fixed widths. The Wigner density of each particle is derived through a Fourier transformation of the density matrix. The collective many-body behavior is captured by constructing the n-body Wigner density as a direct product of individual particle densities, and its evolution follows from a generalized Ritz variational principle. In contrast to mean-field approaches, which simplify the dynamics of nucleons by integrating out the phase-space correlations between them, hence reducing to single-particle propagation in a mean-field potential, the QMD approach preserves these correlations and fluctuations, a feature that is clearly essential for the dynamical cluster formation.

  ii) In the Parton-Hadron-String-Dynamics (PHSD) [5] the degrees of freedom of the strongly interacting medium are off-shell hadrons and off-shell massive quasi-particles representing the deconfined quarks and gluons of the QGP phase, which is created if the local energy density is larger than a critical value of $\epsilon_c \approx 0.5$ GeV/fm^3. In the Kadanoff-Baym transport theory the propagation of these off-shell degrees of freedom and their corresponding spectral functions is described by means of the generalized Cassing-Juchem equations derived in test-particle representation. In PHSD the elementary hadronic reactions for particle production are taken from its early Hadron-String-Dynamics (HSD) model [6]. The interaction among partons in the QGP phase is described within the framework of the Dynamical Quasi-Particle Model (DQPM). In this model, quarks and gluons are depicted as massive, strongly interacting quasi-particles, whose properties, including mass pole positions and spectral widths, are computed via the real and the imaginary components of the parton self-energies, and their T and μ_B dependence is tuned to lattice QCD.

For more details of the PHQMD model we refer to [1-3] and reference therein. We proceed now to describe the dynamical production of deuterons in PHQMD.

Potential mechanism - In PHQMD the formation of clusters through potential interaction among nucleons has been initially investigated employing the original Minimum-Spanning-Tree (MST) recognition algorithm [2,3]. In this study we employ an improved version of MST, coined *advanced* MST (aMST), which is essential to overcome a numerical artifact which leads to suppression of stable clusters during the PHQMD time evolution (details in ref. [1]). The key computational issue can be addressed by "freezing" the internal dynamics of a cluster once its nucleons are no longer interacting (neither by collisions nor potential interactions) with other hadrons outside the cluster. This freezing or "stabilization" process demands modifying the "collision history" file containing baryon positions and momenta over time at the end of the complete PHQMD evolution, hence preventing any affection to the reaction dynamics. The procedure involves the following steps which are highlighted in fig. 1 - showing the multiplicity of $A = 2$ clusters at mid-rapidity at four RHIC Beam Energy Scan (BES) energies:

  1) Nucleons can only form a cluster after their final elastic or inelastic collision. At each time step, positions and momenta are recorded, and clusters are identified using the standard MST algorithm (thin dashed black line).

  2) Clusters must exhibit negative binding energy ($E_B < 0$) in order to be considered as bound ones. Therefore, after MST identification, only clusters meeting this criterion must be selected (dash-dotted red line).

3) In PHQMD energy is strictly conserved and cluster nucleons are maximally separated from other nucleons with a specified radius. However, due to the fact that the potential energy changes, when performing Lorentz boost forward and backward between the laboratory and the cluster rest frame, the binding energy of a cluster may transiently become positive, leading to unnatural disintegration. To prevent this numerical artificial, the internal degrees of freedom must be frozen.

4) Semi-classical approaches, such as QMD, may also lead to artificial disintegration of "bound" clusters with negative binding energy. To address this, those nucleons, which have spontaneously evaporated, are reintegrated into the belonging cluster.

In fig. 1 the result after including the 3) and 4) steps is represented by the solid green line and, finally, the mid-rapidity distribution of bound ($E_B < 0$) "potential" deuterons as function of time is depicted in fig. 1 by the solid green line with full squares. It is clearly visible that the "stabilization" procedure ensures that fragments remain stable and bound over time. The effect of freezing internal cluster dynamics is significant at increasing beam energies, while it remains minimal at lower ones.

Kinetic mechanism - An important novelty of this study concerns the implementation of deuteron $\pi NN \leftrightarrow \pi d$ and $NNN \leftrightarrow Nd$ reactions in the collision integral of PHQMD, which is originally early from the PHSD transport approach. This is physically motivated by the fact that these are the dominant reactions for the production of deuterons in HICs due to their large cross sections, $\sigma_{tot} \approx 200$ mb, compared to the sub-dominant channel $NN \leftrightarrow d\pi$ with $\sigma_{tot} \approx 10$ mb. To implement such reaction we employ the so-called covariant rate formalism, which as been advanced in ref. [9] to describe baryon-
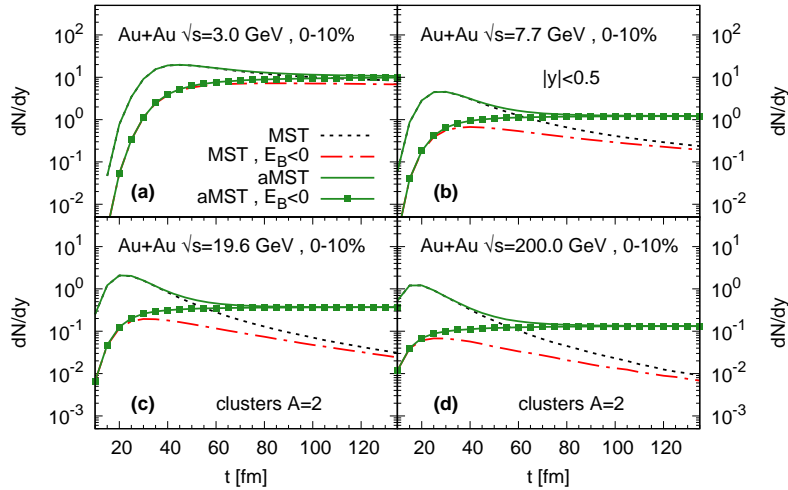

Fig. 1. – Multiplicity of $A = 2$ clusters at mid-rapidity in PHQMD Au+Au central collisions at four RHIC BES energies: (a) $\sqrt{s} = 3$ GeV,(b) $\sqrt{s} = 7.7$ GeV, $\sqrt{s} = 19.6$ GeV, (d) $\sqrt{s} = 200$ GeV. The different lines indicate the various "stabilization" steps described in the text to identify the potential deuterons: standard MST (dashed black), MST with $E_B < 0$ (dash-dotted red), advanced MST (solid green) and advanced MST with $E_B < 0$ (solid green line with full squares).

antibaryon annihilation and inverse production via multi-meson fusion within the PHSD approach. As explained in detail in ref. [1] the numerical implementation of the multi-particle reactions requires the division of the space grid in sufficiently small cells with unit volume ΔV, where collisions among particles in the same cell can be sampled at each mesh time Δt by means of the stochastic method. Here we report the resulting probabilities for the production and disintegration of deuteron through pion (nucleon) catalysis which we employ in the stochastic method. The collision probability for the $\pi(N)NN \to d\pi(N)$ reaction in the unit volume ΔV and the unit time Δt is given by

$$(1) \qquad P_{3,2} = F_{spin}F_{iso}\frac{E_d^f E_{\pi(N)}^f}{2E_{\pi(N)}^i E_N^i E_N^i}\frac{P_{2,3}}{\Delta V}\frac{R_2(\sqrt{s}, m_d, m_{\pi(N)})}{R_3(\sqrt{s}, m_{\pi(N)}, m_N, m_N)} \, .$$

One can see that, under the detailed balance assumption and requiring the transition amplitude to depend only on $\sqrt{s}$, the production probability eq. (1) depends linearly on the probability for the inverse $d\pi(N) \to \pi(N)NN$ process, which is given by

$$(2) \qquad P_{2,3} = \sigma_{tot}^{2,3}(\sqrt{s})v_{rel}\frac{\Delta t}{\Delta V} \, ,$$

where v_{rel} is the relative velocity and $\sigma_{tot}^{2,3}$ is the total inelastic cross section, respectively, for d disintegration by incident π or N as function of the center-of-mass energy of the collisions $\sqrt{s}$. The cross section has been derived from a fit to available experimental data as described in the Appendix A of ref. [1]. In eq. (1) it appears the ratio among the energies of initial (i) and final (f) particles as well as the ratio between the two-body and three-body phase space integral, which can be parametrized as function of $\sqrt{s}$ and particle masses. F_{spin} and F_{iso} denote the factors arising from summing, respectively, over the internal spin and the isospin quantum numbers in the transition amplitude to compute the total cross section $\sigma_{tot}^{2,3}$. For both nucleon and pion catalysis $F_{spin} = 3/4$. The isospin factor F_{iso} is , instead, computed from the Fourier coefficients for those channels which are allowed by total isospin conservation. All the values of F_{iso} for each implemented reaction channel are collected in Appendix D of ref. [1]. All deuteron reactions have been firstly tested in a static "box" environment, where the numerical results from numerical collision criteria have been checked with analytic solutions from rate equations and the detailed balance condition has been verified. The details are reported in sect. IV of ref. [1]. Subsequently, we performed realistic simulations and studied the impact of opening new channels allowed by total isospin conservation on the production of d by hadronic collisions. In fig. 2 left plot, the yield of "kinetic deuterons" at mid-rapidity in Au+Au central collisions at $\sqrt{s} = 7.7$ GeV from all implemented reactions (solid black line) is confronted to the case of reactions pion charge exchange (dash-dotted orange line). Compared also to the STAR data (full dot) the former case shows an enhancement of about 50% than the latter one.

Finite-size effects - In Quantum Mechanics the deuteron is a broad *pn* bound system with a radius of about 2 fm. The expression for stochastic probabilities eq. (2) and eq. (1) derived within the covariant rate formalism assume the deuteron to be a point-like particle. Therefore, it is reasonable to conclude that the deuteron, being an extended quantum object in coordinate space whose constituing *pn* share a small relative momentum, cannot be produced as a point-like hadron. We have taken this into account by modeling some finite-size effects and we have considered three possible scenarios:

I) We have introduced an excluded-volume condition which suppresses the formation of kinetic deuterons in the presence of surrounding hadrons. The exclusion radius R_d is a physical parameter which we have tuned to the root-mean-square radius through the Deuteron Wave Function (DWF) in coordinate space $|\phi_d(r)|^2$.

II) Similarly to what has been done in ref. [10], we have taken into account also quantum properties by projecting the relative momentum of the NN-pairs on the DWF in momentum space $|\phi_d(p)|^2$, which (normalized to unity) we used as a probability distribution to select the pn bound pairs in $\pi(N)NN \to d\pi(N)$ reactions.

III) We have studied the impact of including finite-size effects both in coordinate space I) and in momentum space II) on the yield kinetic deuterons.

In fig. 2 right plot, one can see that the inclusion of these finite-size effects leads to a significant reduction of mid-rapidity kinetic d in Au+Au central collisions at $\sqrt{s} = 7.7$ GeV. Surprisingly, the excluded-volume (solid red line) and the momentum projection (dashed blue line) at $|y| < 0.5$ give a similar suppression of about a factor 3. However, we find that at higher rapidities their effect leads to a different dN/dy of kinetic deuterons at increasing collision energies (fig. 10 ref. [1]). Finally, applying both effects together the yield of d is suppressed by an additional factor of two (green line with filled squares).

3. – Results

In this section we present PHQMD rapidity distribution dN/dy - fig. 3 - and transverse momentum (p_T) spectra - fig. 4 - for "potential" deuterons from aMST (dashed green line) and "kinetic" deuterons (solid red line) in Pb+Pb central collisions at two CERN SPS energies $E_{Lab} = 40$ AGeV and $E_{Lab} = 158$ GeV. The various columns denote the three different models of finite-size effects described above. In particular, we find that the III) scenario leads to a strong suppression of kinetic d with respect to potential ones within the full rapidity range. Furthermore, the combination of both production mechanisms
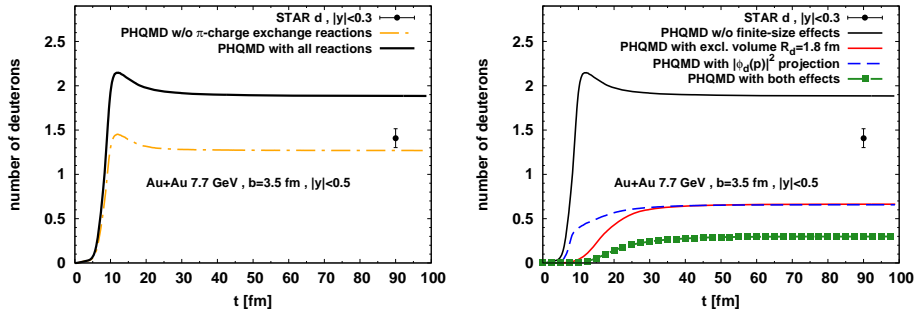

Fig. 2. – Time evolution of mid-rapidity "kinetic" deuteron number in Au+Au central collisions at $\sqrt{s} = 7.7$ GeV. Left: PHQMD results with all reaction channels for $N-$ and $\pi-$catalysis implemented (thick black line) are compared to those where π charge exchange reactions are neglected (dash-dotted orange line). Right: Impact of finite-size effects on kinetic deuteron production. The black solid line is the same as in the right plot without finite-size effects. The other three lines correspond to the three different models: I) excluded-volume (solid red), II) momentum projection on DWF (dashed blue), III) both effects (green line with filled squares). The full black point in both figures represents experimental data from STAR at mid-rapidity [11].
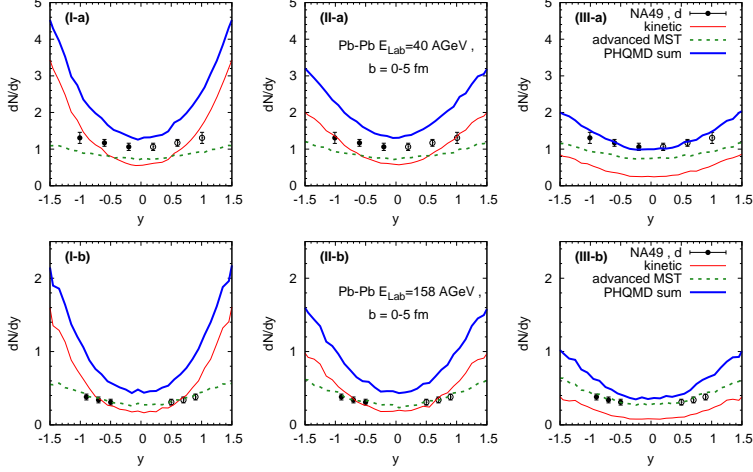
Fig. 3. – PHQMD dN/dy distributios of aMST identified potential d (dashed green line), kinetic d (solid red line) and total d (thick solid blue line) in Pb+Pb central collisions at $E_{Lab} = 40$ AGeV (upper plots) and $E_{Lab} = 158$ AGeV (lower plots). The three columns denote the studied scenarios for finite-size effects in kinetic d production: I) excluded-volume (left), II) momentum projection (middle), III) both effects (right). The full dots are the data from NA49 [12].

(solid blue line) provides good description of the available experimental data from NA49 collaboration (full dots) [12]. Such agreement is visible only looking at the dN/dy profile, whereas in the case of the p_T-spectra at mid-rapidity it is not possible to distinguish among the different models. In ref. [1] we have performed PHQMD simulations at higher energies and computed dN/dy and p_T-spectra of potential and kinetic deuterons with both finite-size effects (III) at RHIC BES range from $\sqrt{s} = 7.7$ GeV up to $\sqrt{s} = 200$ GeV. We have found that the potential contribution is dominant compared to the collisional one and, finally, we have compared our results to the STAR measurements at mid-rapidity [11] finding very good agreement.

4. – Conclusions

In this contribution we discussed about two dynamical mechanisms for d production in HICs within the PHQMD transport approach and we reported the main results of ref. [1]. Future developments within this model are still ongoing and regards the analysis of other light (hyper-)nuclei using the novel advanced MST method to study the properties of nuclear matter at finite temperature and density. The investigation of cluster formation in HICs remains an active area of research. Numerous theoretical models have been proposed, each based on distinct production mechanisms. Discrimination between these models can be achieved reducing the experimental uncertainties as well as measuring novel observables at present and forthcoming facilities. This is crucial also for obtaining useful information in the comprehension of neutron stars and in the quest of Dark Matter searches in high-energy cosmic rays. Moreover, it is important to emphasize the impact of quantum properties on cluster formation, which can be studied within the framework of open quantum systems theory. This ongoing pursuit underscores the complexity of the phenomena involved and the importance of advancing our understanding of cluster production in nuclear collisions.
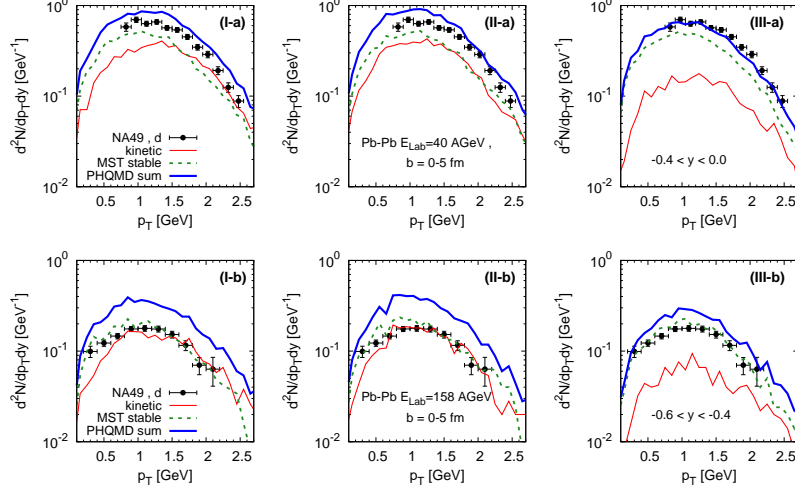
Fig. 4. – PHQMD $dN/dp_T dy$ spectra of aMST, kinetic and total d in Pb+Pb central collisions at $E_{Lab} = 40$ AGeV (upper plots) and $E_{Lab} = 158$ AGeV (lower plots). Line styles and colors are the same of fig. 3, as well as the three column separation for finite-size effects on kinetic d. The y-range of PHQMD results and NA49 data [12] (full dots) is indicated on the right plots.

REFERENCES

[1] COCI G., GLÄSSEL S., KIREYEU V., AICHELIN J., BLUME C., BRATKOVSKAYA E., KOLESNIKOV V. and VORONYUK V., *Phys. Rev. C*, **108** (2023) 014902, arXiv:2303.02279 [nucl-th].

[2] AICHELIN J., BRATKOVSKAYA E., LE FÈVRE A., KIREYEU V., KOLESNIKOV V., LEIFELS Y., VORONYUK V. and COCI G., *Phys. Rev. C*, **101** (2020) 044905, arXiv:1907.03860 [nucl-th].

[3] GLÄSSEL S., KIREYEU V., VORONYUK V., AICHELIN J., BLUME C., BRATKOVSKAYA E., COCI G., KOLESNIKOV V. and WINN M, *Phys. Rev. C*, **105** (2022) 014908, arXiv:2106.14839 [nucl-th].

[4] AICHELIN J., *Phys. Rep.*, **202** (1991) 233.

[5] CASSING W. and BRATKOVSKAYA E. L., *Nucl. Phys. A*, **831** (2009) 215, arXiv:0907.5331 [nucl-th].

[6] CASSING W. and BRATKOVSKAYA E. L., *Phys. Rep.*, **308** (1999) 65.

[7] SMASH COLLABORATION (OLIINYCHENKO D. *et al.*), *Phys. Rev. C*, **99** (2019) 044907, arXiv:1809.03071 [hep-ph].

[8] SMASH COLLABORATION (STAUDENMAIER J. *et al.*), *Phys. Rev. C*, **104** (2021) 034908, arXiv:2106.14287 [hep-ph].

[9] CASSING W., *Nucl. Phys. A*, **700** (2002) 618, arXiv:nucl-th/0105069.

[10] SUN K. J., WANG R., KO C. M., MA Y. G. and SHEN C.,, arXiv:2106.12742 [nucl-th].

[11] STAR COLLABORATION (ADAM J. *et al.*), *Phys. Rev. C*, **99** (2019) 064905, arXiv:1903.11778 [nucl-ex].

[12] NA49 COLLABORATION (ANTICIC T. *et al.*), *Phys. Rev. C*, **94** (2016) 044906, arXiv:1606.04234 [nucl-ex].